Carbohydrate Polymers 86 (2011) 1151–1156

Contents lists available at ScienceDirect

Carbohydrate Polymers

journal homepage: www.elsevier.com/locate/carbpol

Enhanced mechanical properties of novel chitosan nanocomposite fibers

Jiahui Chen[a], Leslie S. Loo[a,*], Kean Wang[b]

[a] School of Chemical and Biomedical Engineering, Nanyang Technological University, Singapore 637459, Singapore
[b] Department of Chemical Engineering, The Petroleum Institute, Abu Dhabi, United Arab Emirates

ARTICLE INFO

Article history:
Received 18 January 2011
Received in revised form 27 May 2011
Accepted 6 June 2011
Available online 12 June 2011

Keywords:
Chitosan
Polyhedral oligomeric silsesquioxanes
Single-walled carbon nanotubes
Composite fibers
Mechanical properties

ABSTRACT

Novel chitosan (CS) nanocomposite fibers based on polyhedral oligomeric silsesquioxane (POSS) and single-walled carbon nanotubes (SWNT) have been successfully prepared by wet-spinning. Octa-ammonium (OA) and octa nitro phenyl silsesquioxane (ONPS) POSS were used in the study. The effect of SWNT and POSS concentration on the morphology and tensile properties of the nanocomposite fibers were investigated. The nanocomposites exhibited superior overall mechanical performance (strain at break, tensile stress, Young's modulus, toughness) at low nano-filler loadings compared to pure chitosan. This was attributed to well-dispersed filler morphology as demonstrated by SEM results.

1. Introduction

Chitosan (CS) has attracted much attention in research and industry because it is nontoxic, biocompatible, bacteriostatic and fungistatic (d'Ayala, Malinconico, & Laurienzo, 2008). As a linear natural polysaccharide which comprises β-(1–4)-linked D-glucosamine (deacetylated unit) and N-acetyl-D-glucosamine (acetylated unit), CS has a number of commercial and biomedical applications, given its abundance in the natural environment (Aranaz et al., 2009). It can be produced very cheaply since it is derived by the deacetylation of chitin and chitin is the second most abundant biopolymer in nature next to cellulose. All these features render CS a promising material for wide spread applications.

CS is available in a wide range of molecular weights and degrees of deacetylation, which are the main factors affecting the particle size, particle formation and aggregation (Tiyaboonchai, 2003). One of the applications of CS includes water processing engineering as a part of a filtration process. CS causes the fine sediment particles to bind together and is subsequently removed with the sediment during sand filtration. CS also removes phosphorus and heavy minerals (Gamage & Shahidi, 2007; Guibal, 2004). Another application of CS is as a plant growth enhancer to enhance the ability of plants to defend against fungal infections (Suchada Boonlertnirun, 2008). In the biomedical field, CS is used in bandages as an agent for blood clotting to stop bleeding (Burkatovskaya et al., 2006), as well as in the form of nanoparticles for drug delivery systems in parenteral and ocular administration (Tiyaboonchai, 2003).

Polyhedral oligomeric silsesquioxanes (POSS) are new organic–inorganic hybrid materials that have received extensive attention for their processability, cage-like framework, and compatibility with other polymers. The structural formula of POSS is shown in Fig. 1 and is usually presented as $R_8Si_8O_{12}$, where the functional group R could be hydrogen, alkyl, aryl arylene groups etc. POSS are accessible by hydrolysis of trifunctional $RSiY_3$ molecules (Agaskar, 1991; Martynova & Korchkov, 1983; Strachota et al., 2007) and can be modified by a number of substitution reactions. Thus, functionalized silsesquioxanes have become available and these are very interesting precursors to organolithic macromolecular materials (Agaskar, 1989, 1990; Yuchs & Carrado, 1996) or hybrid inorganic–organic materials (Baney, Itoh, Sakakibara, & Suzuki, 1995; Loy & Shea, 1995; Sellinger & Laine, 1996a, 1996b). Other than the silsesquioxanes with silicon–oxygen frameworks, different hetero- and metalla-siloxanes (Murugavel, Voigt, Walawalkar, & Roesky, 1996) have been prepared, such as alumino-, titana-, and galliumsilsesquioxanes where one (Feher, 1986; Feher, Budzichowski, Blanski, Weller, & Ziller, 1991; Feher, Budzichowski, Rahimian, & Ziller, 1992; Feher, Budzichowski, & Weller, 1989; Feher & Weller, 1990; Feher, Weller, & Ziller, 1992; Ohshita et al., 1991) or several silicon atoms are replaced (Marcolli & Calzaferri, 1999).

As the fine control of the polymer morphology at the nanoscale level provides opportunities for the design of new materials, hybrid

* Corresponding author at: School of Chemical and Biomedical Engineering, Nanyang Technological University, N1.2 B1-12, 62 Nanyang Drive, Singapore 637459, Singapore. Tel.: +65 67906737; fax: +65 67947553.
E-mail address: ssloo@ntu.edu.sg (L.S. Loo).

0144-8617/$ – see front matter © 2011 Elsevier Ltd. All rights reserved.
doi:10.1016/j.carbpol.2011.06.013

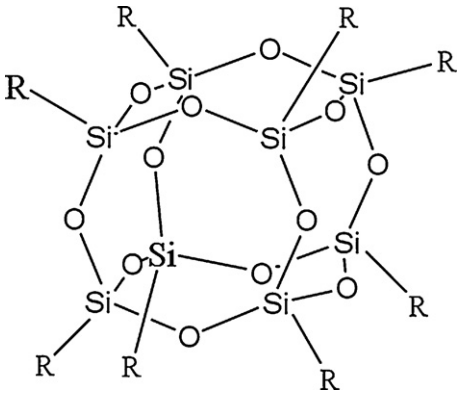

Fig. 1. The basic structure of POSS.

polymers with incorporated organosiloxane compounds have been recently studied (Cornelius & Marand, 2002). A typical hybrid material will contain a cross-linked inorganic phase bound (often covalently) with an organic phase (Haddad & Lichtenhan, 1996). This polymer-POSS compatibility is formed by the formation of covalent and non-covalent bonds between POSS tethers and polymer chains. Due to the rigidity of the cage like structure of Si_8O_{12} and the flexibility of the tethers, POSS molecules are well-dispersed nanofillers, affecting the morphology and mechanical stability of POSS-reinforced polymer matrices under elevated temperature and deformation.

POSS molecules can be incorporated into polymer systems through blending, grafting or copolymerization. Blends of POSS and polycarbonate (PC) have been reported to possess better mechanical and thermal properties (Zhao & Schiraldi, 2005). POSS acts as a nano-scale filler modifying the PC matrix with improved properties. POSS can exhibit enhanced compatibility resulting from favorable interactions between its organic substituents and matrix polymer. It is generally believed that nanoscale POSS domains with ordered and self-assembled features in a polymer matrix are highly desirable and can lead to the observed improvements in material properties. POSS/poly(ethylene terephthalate) nanocomposite fibers were reported to have better tensile strength and modulus (Kim, Bang, Choi, & Yoon, 2008). Furthermore, the melt blending of POSS and polypropylene resulted in better mechanical performance, with higher elastic modulus as well as higher elongation at break (Fina, Tabuani, & Camino, 2010). POSS blended with poly(2,6-dimethyl-1, 4-phenylene oxide)/polyamide 6 has also led to enhancement in mechanical properties and thermal properties (Li, Zhang, Wang, & Ji, 2009).

POSS has been used to modify the morphology of CS membranes and consequently their permeability (Tishchenko & Bleha, 2005). Bleha et al. studied the effect of POSS functionality on the morphology of thin CS film (Bleha, Tishchenko, Pientka, & Brus, 2004). The preparation and diffusion permeability of CS-amino-POSS and CS-epoxy-POSS membranes were studied as well (Strachota, Tishchenko, Matejka, & Bleha, 2001). However, to the author's knowledge, there has been no study on CS-POSS fibers and their mechanical properties. Hence one of the objectives of this work is to incorporate POSS into CS matrix to synthesize composite fibers with enhanced mechanical properties.

Carbon nanotubes (CNT) possess excellent mechanical properties (Allaoui, Bai, Cheng, & Bai, 2002), as well as electrical (Baughman, Zakhidov, & de Heer, 2002) and thermal conductivity (Biercuk et al., 2002). They are classified into single-walled carbon nanotubes (SWNT) and multi-walled carbon nanotubes (MWNT). SWNT consist of a single layer of graphite sheet wrapped around in a cylindrical shape while MWNT consist of multi-layers of graphite wrapped on top of each layer to form a tubular structure. A single-walled nanotube can exhibit a tensile strength of up to 45 GPa whereas the highest grade steel alloy used in the construction of mega-structures can only withstand up to 2 GPa. The current carrying capacity of carbon nanotubes is estimated to be around 10^9 A cm^{-2} while the most expensive copper wire will burn out at a much smaller capacity of 10^6 A cm^{-2}. Due to its excellent properties, CNT has been blended with many polymers to enhance their mechanical properties (Coleman, Khan, Blau, & Gun'ko, 2006), such as SWNT/nylon composite fiber (Gao et al., 2005) and CNT/epoxy composite fiber (Guo, Chen, Gao, Song, & Shen, 2007). CNT/CS composite fibers were also reported to have improved mechanical properties. Using centrifugation to improve dispersion of CNT in CS matrix has resulted in higher Young's modulus and higher tensile strengths. However, the strain was much less than pure CS (Shin et al., 2006; Spinks et al., 2006). Another objective of this work is to obtain SWNT/CS nanocomposites with enhanced overall mechanical properties (e.g. tensile stress, strain at break, Young's modulus and toughness).

2. Experiment

2.1. Materials

Chitosan (CS) was obtained from Bannawach Bioline Company in Thailand. The CS was formed by the deacetylation of chitin from crab shells and is fully deacetylated (measured molecular weight is 187,260). The basic properties of single wall carbon nanotube (SWNT) are shown in Table 1. The two types of POSS selected for this experiment are octa ammonium (OA) and octa nitro phenyl silsesquioxane (ONPS). Their structures are shown in Fig. 2. OA was supplied by Hybrid Plastics, Inc., and ONPS was supplied by Mayaterials Inc. Acetic acid and methanol were supplied by Sigma Aldrich and used as received. 27.8 ml of 50% NaOH from Aik Moh Paints & Chemical Pte. Ltd. Singapore, was diluted to 500 ml by adding to make up a solution of 1 M NaOH.

2.2. Methodology

2.2.1. Preparation of CS solution

0.15 g CS was dissolved in 10 ml 1% acetic acid solution. CS is readily soluble in most aqueous acid solutions, because of the basicity of the primary amine groups. A magnetic stirrer was used to stir the mixture for 4 h at a constant rate of 700 rpm at room temperature to ensure the complete dissolution of the CS. POSS or SWNT was then added slowly into the solution. Such progressive addition would ensure more homogenous dispersion of the nano-fillers in the CS matrix. The final mixture was stirred overnight (24 h). Care was taken to remove all air bubbles. Different concentrations (w/w%) of SWNT or POSS with CS was prepared: 1% (0.0015 g), 3% (0.0045 g), 5% (0.0075 g), 7% (0.0105 g) and 9% (0.0135 g).

2.2.2. Fabrication of the fibers

The CS matrix nanocomposite fibers were fabricated by wet spinning. Melt spinning is not very suitable since CS will degrade at high temperatures. 10% NaOH was flowed from a beaker through an epoxy-cured silicon tube (length: 50 cm, inside diameter: 0.8 mm) into the coagulation bath using a peristaltic pump. The dope, which was the CS/POSS or CS/SWNT mixture in acetic acid prepared in (1), was injected into the silicon tube via a syringe pump at a rate

Table 1
The basic properties of SWNT used in the experiment.

	Outer diameter (nm)	Length (μm)	Purity
SWNT	<2	5–15	>90 wt%

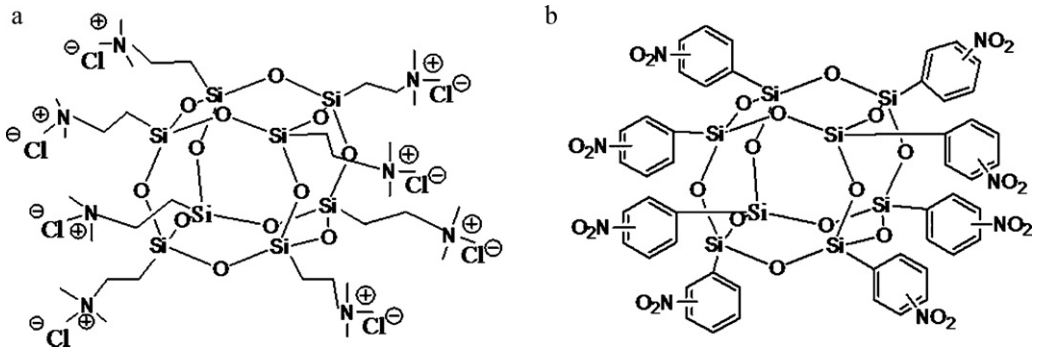

Fig. 2. The chemical structures of the two kinds of POSS: (a) OA and (b) ONPS.

of 5 ml/min. Upon contact of the dope with the NaOH solution, POSS/CS or SWNT/CS precipitated out as fiber. The fiber obtained was collected in a petri-dish filled with 10% NaOH and was subsequently transferred to water and allowed to stand for at least 15 min. The fiber was then transferred into methanol solution for another 10 min before drying. The methanol allows quick drying of the composite fiber.

2.3. Characterization

OA/CS, ONPS/CS and SWNT/CS fibers were subjected to tensile tests in the laboratory at room temperature. Tensile were conducted using the Tensile Testing Device by Sensorcraft Technology. It was connected to the data acquisition software DC 104R that recorded the stress load and strain of each sample. An elongation rate of 0.06 mm/s was used. The mean of at least 6 samples was reported. Toughness was calculated by determining the area under the stress–strain curve. A phase microscope was used to determine the thickness and to provide an image of the fiber sample. Micrographs were from scanning electron microscope (SEM) were obtained with JEOL JSM-6390LA Analytical Electron Scanning Microscope.

3. Results and discussion

3.1. OA/CS composites

Fig. 3a–d shows the stress at fracture, strain at fracture, Young's modulus and toughness respectively of OA/CS nanocomposites at various filler loadings. The amount of stress that the samples can handle generally increased as the loading of OA increased, until it reached a maximum at 7 wt%, beyond which it decreased. A similar trend was seen in the bar charts for strain, Young's modulus and toughness. The highest strain at fracture, Young's modulus and toughness were also observed at the OA loading of 7 wt%.

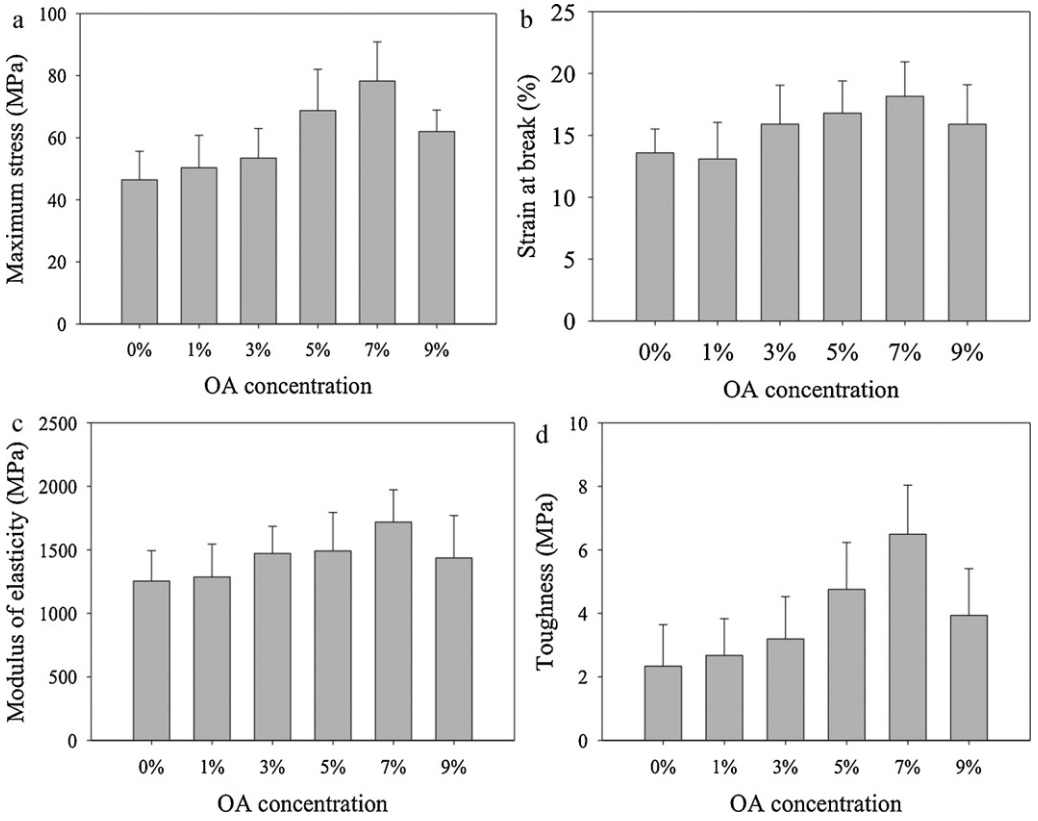

Fig. 3. The mechanical properties of OA/CS composites as a function of OA concentration: (a) maximum stress, (b) strain at break, (c) Young's modulus, and (d) toughness.

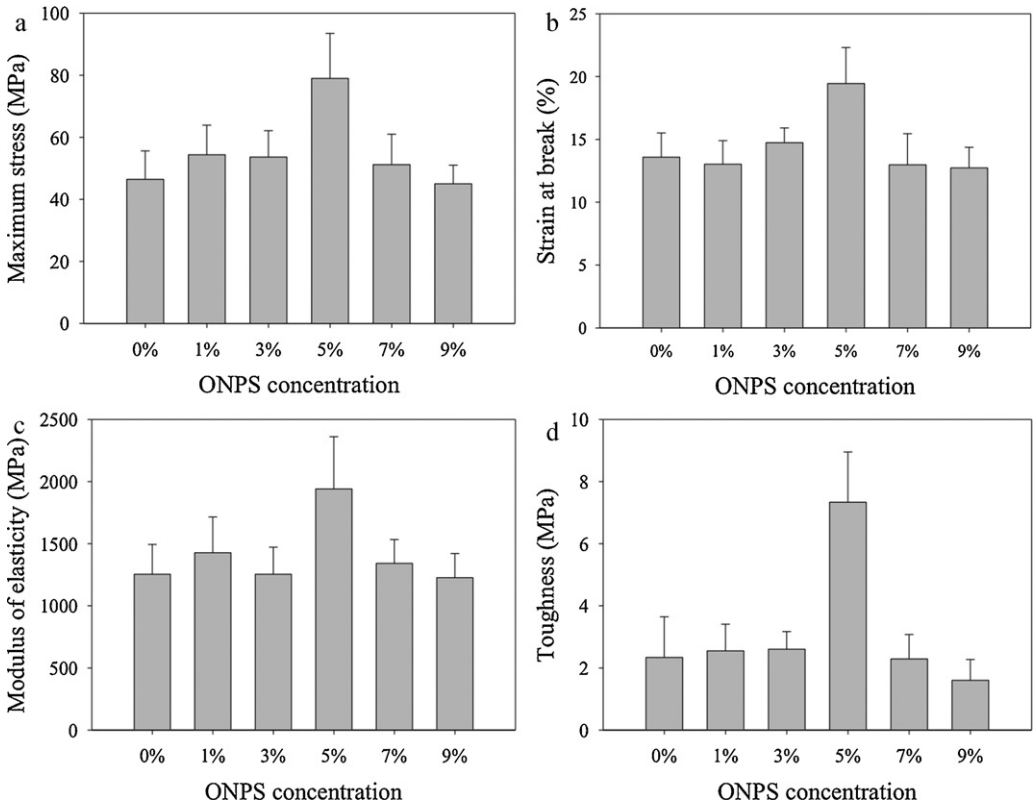

Fig. 4. The mechanical properties of ONPS/CS composites as a function of ONPS concentration: (a) maximum stress, (b) strain at break, (c) Young's modulus, and (d) toughness.

3.2. ONPS/CS composites

Fig. 4a–d shows the stress at fracture, strain at fracture, Young's modulus and toughness respectively of ONPS/CS composites for different ONPS loadings. Similar to OA/CS data, the stress at fracture data generally showed an increasing trend with increasing amounts of ONPS up to 5%, after which it decreased. The trend is generally similar for the other properties. It is seen

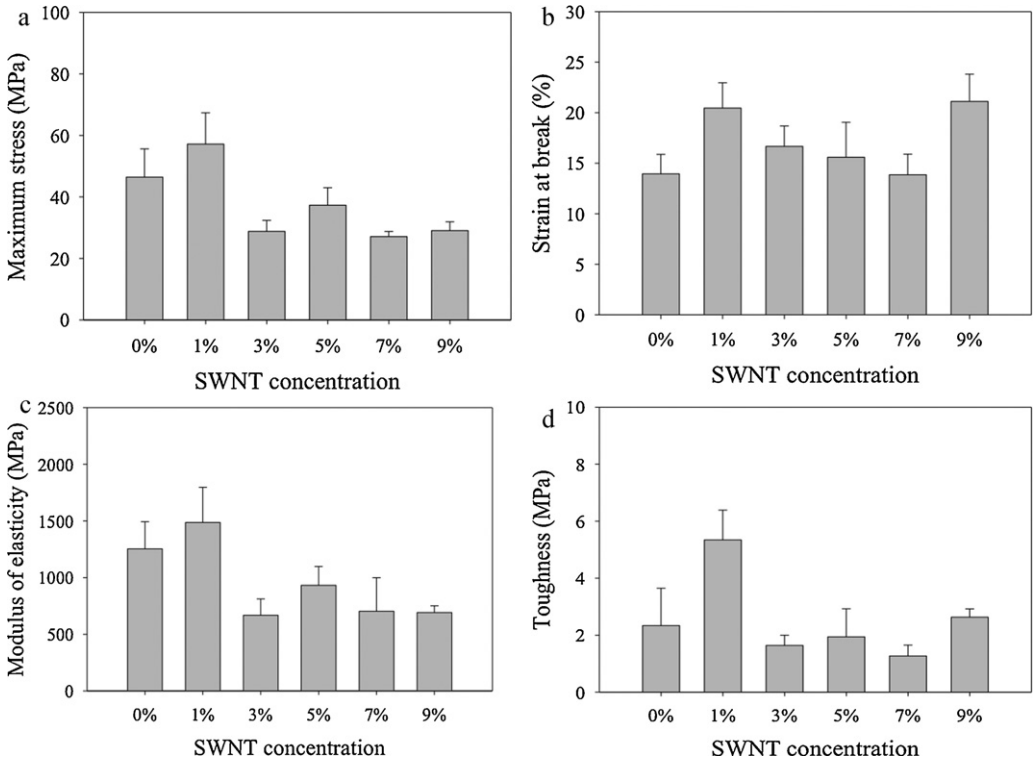

Fig. 5. The mechanical properties of SWNT/CS composites as a function of SWNT concentration: (a) maximum stress, (b) strain at break, (c) Young's modulus, and (d) toughness.

that 5 wt% loading of ONPS in CS resulted in best mechanical performance.

3.3. SWNT/CS composites

Fig. 5a–d shows the stress at fracture, strain at fracture, Young's modulus and toughness of SWNT/CS composites. It is seen that 1 wt% loading of SWNT in CS resulted in the highest stress at fracture among all the weight samples, an increase of 17% over pure CS. The increase in strain was calculated to be 27%. Further increase in SWNT loading beyond 1 wt% SWNT resulted in a decrease in stress at fracture of the fibers. The highest strain at fracture, Young's modulus and toughness were also observed at the SWNT loading of 1 wt%.

Fig. 6a–c shows the images of the fractured samples obtained from SEM for 7 wt% OA, 5 wt% ONPS and 1 wt% SWNT respectively. From the images, it could be seen that the cross-sectional area of the fibers were approximately circular and hence the fibers could be approximated to be cylindrical. Since the size of POSS particles are very small, ranging from 1 to 3 nm, the pores within the structure could be indication of POSS particles integrated within the CS matrix which detached during fracture, described as particle-matrix debonding during deformation by Kopesky, McKinley, and Cohen (2006). The even distribution of pores throughout the cross-section could imply that the POSS domains were evenly distributed through the fracture surface.

Generally, the fibers stress at fracture is also the ultimate stress for CNT. Upon reaching the point of ultimate stress, there was no sign of any further elongation before fracture. This could be attributed to the small dimensions of the fibers that caused instability during the initial stage of neck formation and hence, fracture to take place easily.

The stress at fracture and toughness of the composites increase with increasing amount of loading for all three types of fillers. This is in accordance to the fact that the addition of POSS or SWNT results in nanocomposites which are mechanically stronger as noted by Song, Geng, and Li (2006). However, a maximum amount of stress attained by the fibers is achieved with a certain amount of filler, beyond which the stress would decrease as more filler is added. For the POSS/CS nanocomposites, this could be due to the interference of POSS molecules with the CS matrix as more POSS is added, hence disrupting the structure and causing the fibers to fracture at a smaller load amount. As reported by Kopesky et al. (2006), larger POSS crystallites weakened the material.

Song et al. (2006) also reported that an increase in strain could be due to a better stress transfer mechanism between the two components in the nanocomposite during tensile deformation. The POSS that they used, however, did not lead to a significant increase in the Young modulus of the nanocomposites (less than 5% increase over that of pure CS). Our results showed a significant improvement in both strain to break and Young's modulus of the POSS/CS nanocomposites, indicating the importance of good interfacial interactions between the nano-filler and polymer matrix.

For SWNT, the addition of 1 wt% saw an increase in the stress, Young modulus and toughness of the nanocomposite. However, the mechanical properties of the fibers worsened with increasing amounts of CNT. This could be due to the fact that as more CNT were added, the chances of non-alignment of the CNT increase, hence weakening the composite structure instead of strengthening it. Spinks et al. also reported that large CNT aggregates were also not effective in reinforcing the material (Spinks et al., 2006). This could explain the decrease in stress, Young's modulus and toughness at higher nano-filler content. Spinks et al. (2006) observed that the Young's modulus of the CNT/CS composite increased while the elongation at break decreased as compared to neat CS. In our work, however, the Young's modulus and strain at break of 1 wt% SWNT/CS nanocomposite both increased compared to neat CS. The maximum stress of 1% CNT increases 17% over neat CS. The strain at break was 27% higher than that of pure CS, and there is a 15% increase and a 120% increase respectively for the modulus and toughness compared to pure CS. Hence, adding SWNT into CS matrix has resulted in an overall enhancement of the mechanical properties of the composite.

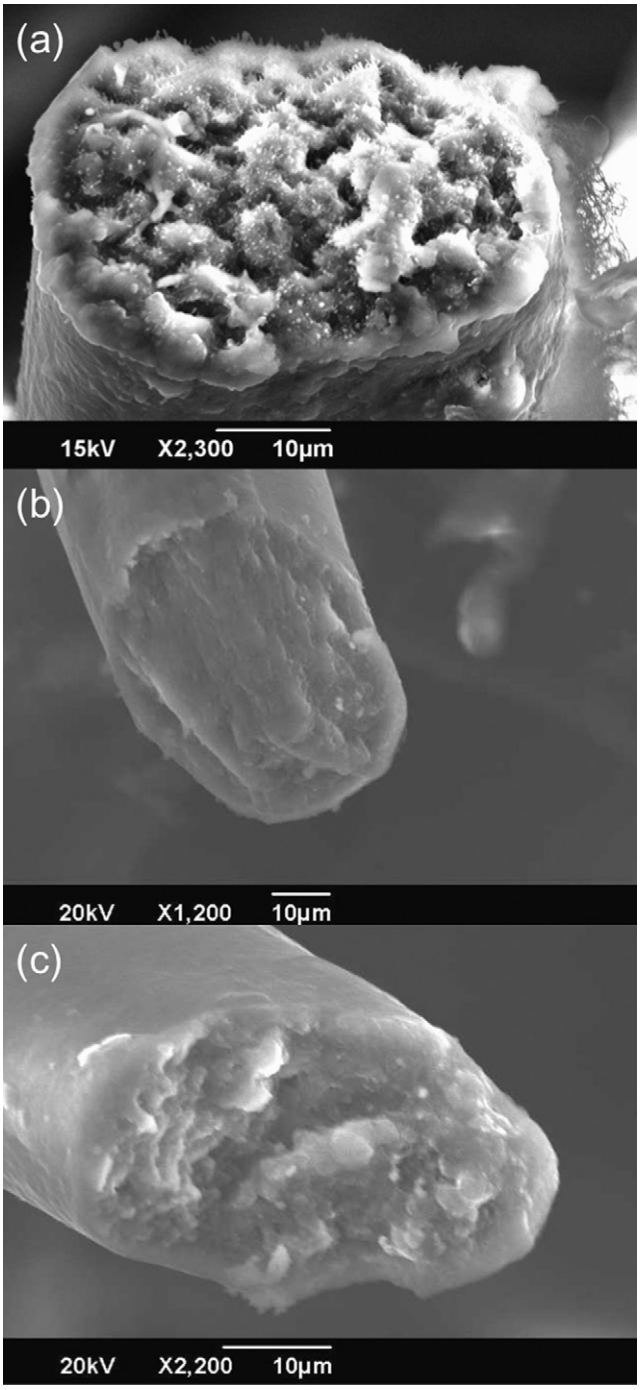

Fig. 6. SEM image of fiber cross-section of (a) 7 wt% OA/CS, (b) 5 wt% ONPS/CS and (c) 1 wt% SWNT/CS nanocomposites.

4. Conclusion

In summary, POSS/CS and SWNT/CS nano-composites with improved mechanical properties have been successfully fabricated

by the wet-spinning method. Fibers fabricated were stiff and rigid as observed by the minimal amount of necking before fracture. The amount of loading resulting in the greatest tensile stress that could be handled was determined to be 7 wt% for OA, 5 wt% for ONPS and 1 wt% for SWNT. An increase in loading resulted in a decrease in tensile strength, which could be due to the disruption of the structure as more filler was introduced. The random alignment of SWNT could be a cause for the weakening of the nano-composite structure. Nonetheless, the improved mechanical properties for CS will serve as a framework for the future development in its application to different fields such as medical and membrane separations.

References

Agaskar, P. A. (1989). Organolithic macromolecular materials derived from vinyl-functionalized spherosilicates: Novel potentially microporous solids. *Journal of the American Chemical Society*, *111*, 6858–6859.

Agaskar, P. A. (1990). Facile, high yield synthesis of functionalized spherosilicates: Precursors of novel organolithic macromolecular materials. *Inorganic Chemistry*, *29*, 1603–11603.

Agaskar, P. A. (1991). New synthetic route to the hydridospherosiloxanes Oh-H8Si8O12 and D5h-H10Si10O15. *Inorganic Chemistry*, *30*, 2707–2708.

Allaoui, A., Bai, S., Cheng, H. M., & Bai, J. B. (2002). Mechanical and electrical properties of a MWNT/epoxy composite. *Composites Science and Technology*, *62*, 1993–1998.

Aranaz, I., Mengibar, M., Harris, R., Panos, I., Miralles, B., Acosta, N., et al. (2009). Functional characterization of chitin and chitosan. *Current Chemical Biology*, *3*, 203–230.

Baney, R. H., Itoh, M., Sakakibara, A., & Suzuki, T. (1995). Silsesquioxanes. *Chemical Reviews*, *95*, 1409–1430.

Baughman, R. H., Zakhidov, A. A., & de Heer, W. A. (2002). Carbon nanotubes—the route toward applications. *Science*, *297*, 787–792.

Biercuk, M. J., Llaguno, M. C., Radosavljevic, M., Hyun, J. K., Johnson, A. T., & Fischer, J. E. (2002). Carbon nanotube composites for thermal management. *Applied Physics Letters*, *80*, 2767–2769.

Bleha, M., Tishchenko, G., Pientka, Z., & Brus, J. (2004). Effect of POSS functionality on morphology of thin hybrid chitosan films. *Designed Monomers & Polymers*, *7*, 25–43.

Burkatovskaya, M., Tegos, G. P., Swietlik, E., Demidova, T. N., P.Castano, A., & Hamblin, M. R. (2006). Use of chitosan bandage to prevent fatal infections developing from highly contaminated wounds in mice. *Biomaterials*, *27*, 4157–4164.

Coleman, J. N., Khan, U., Blau, W. J., & Gun'ko, Y. K. (2006). Small but strong: A review of the mechanical properties of carbon nanotube-polymer composites. *Carbon*, *44*, 1624–1652.

Cornelius, C. J., & Marand, E. (2002). Hybrid silica–polyimide composite membranes: Gas transport properties. *Journal of Membrane Science*, *202*, 97–118.

d'Ayala, G., Malinconico, M., & Laurienzo, P. (2008). Marine derived polysaccharides for biomedical applications: Chemical modification approaches. *Molecules*, *13*, 2069–2106.

Feher, F. J. (1986). Polyhedral oligometallasilsesquioxanes (POMSS) as models for silica-supported transition-metal catalysts. Synthesis and characterization of (C5Me5)Zr[(Si7O12)(c-C6H11)7]. *Journal of the American Chemical Society*, *108*, 3850–3852.

Feher, F. J., Budzichowski, T. A., Blanski, R. L., Weller, K. J., & Ziller, J. W. (1991). Facile syntheses of new incompletely condensed polyhedral oligosilsesquioxanes: [(c-C5H9)7Si7O9(OH)3], [(c-C7H13)7Si7O9(OH)3], and [(c-C7H13)6Si6O7(OH)4]. *Organometallics*, *10*, 2526–2528.

Feher, F. J., Budzichowski, T. A., Rahimian, K., & Ziller, J. W. (1992). Reactions of incompletely-condensed silsesquioxanes with pentamethylantimony: A new synthesis of metallasilsesquioxanes with important implications for the chemistry of silica surfaces. *Journal of the American Chemical Society*, *114*, 3859–3866.

Feher, F. J., Budzichowski, T. A., & Weller, K. J. (1989). Polyhedral aluminosilsesquioxanes: Soluble organic analogs of aluminosilicates. *Journal of the American Chemical Society*, *111*, 7288–7289.

Feher, F. J., & Weller, K. J. (1990). Polyhedral aluminosilsesquioxanes as models for aluminosilicates: Unique synthesis of anionic aluminum/silicon/oxygen frameworks. *Organometallics*, *9*, 2638–2640.

Feher, F. J., Weller, K. J., & Ziller, J. W. (1992). Synthesis and characterization of an aluminosilsesquioxane framework that violates Loewenstein's rule. *Journal of the American Chemical Society*, *114*, 9686–9688.

Fina, A., Tabuani, D., & Camino, G. (2010). Polypropylene–polysilsesquioxane blends. *European Polymer Journal*, *46*, 14–23.

Gamage, A., & Shahidi, F. (2007). Use of chitosan for the removal of metal ion contaminants and proteins from water. *Food Chemistry*, *104*, 989–996.

Gao, J., Itkis, M. E., Yu, A., Bekyarova, E., Zhao, B., & Haddon, R. C. (2005). Continuous spinning of a single-walled carbon nanotube-nylon composite fiber. *Journal of the American Chemical Society*, *127*, 3847–3854.

Guibal, E. (2004). Interactions of metal ions with chitosan-based sorbents: A review. *Separation and Purification Technology*, *38*, 43–74.

Guo, P, Chen, X., Gao, X., Song, H., & Shen, H. (2007). Fabrication and mechanical properties of well-dispersed multiwalled carbon nanotubes/epoxy composites. *Composites Science and Technology*, *67*, 3331–3337.

Haddad, T. S., & Lichtenhan, J. D. (1996). Hybrid organic–inorganic thermoplastics: styryl-based polyhedral oligomeric silsesquioxane polymers. *Macromolecules*, *29*, 7302–7304.

Kim, H.-U., Bang, Y. H., Choi, S. M., & Yoon, K. H. (2008). Morphology and mechanical properties of PET by incorporation of amine-polyhedral oligomeric silsesquioxane. *Composites Science and Technology*, *68*, 2739–2747.

Kopesky, E. T., McKinley, G. H., & Cohen, R. E. (2006). Toughened poly(methyl methacrylate) nanocomposites by incorporating polyhedral oligomeric silsesquioxanes. *Polymer*, *47*, 299–309.

Li, B., Zhang, Y., Wang, S., & Ji, J. (2009). Effect of POSS on morphology and properties of poly(2,6-dimethyl-1,4-phenylene oxide)/polyamide 6 blends. *European Polymer Journal*, *45*, 2202–2210.

Loy, D. A., & Shea, K. J. (1995). Bridged polysilsesquioxanes. Highly porous hybrid organic–inorganic materials. *Chemical Reviews*, *95*, 1431–1442.

Marcolli, C., & Calzaferri, G. (1999). Monosubstituted octasilasesquioxanes. *Applied Organometallic Chemistry*, *13*, 213–226.

Martynova, T. N., & Korchkov, V. P. (1983). Dehydrocondensation of hydrogen-containing cyclosiloxanes. *Journal of Organometallic Chemistry*, *248*, 241–249.

Murugavel, R., Voigt, A., Walawalkar, M. G., & Roesky, H. W. (1996). Hetero- and metallasiloxanes derived from silanediols, disilanols, silanetriols, and trisilanols. *Chemical Reviews*, *96*, 2205–2236.

Ohshita, J., Ohsaki, H., Ishikawa, M., Tachibana, A., Kurosaki, Y., Yamabe, T., et al. (1991). Silicon–carbon unsaturated compounds, 26. Photochemical behavior of 1,4- and 1,5-bis(pentamethyldisilanyl)naphthalene. *Organometallics*, *10*, 880–887.

Sellinger, A., & Laine, R. M. (1996a). Silsesquioxanes as synthetic platforms. 3. Photocurable, liquid epoxides as inorganic/organic hybrid precursors. *Chemistry of Materials*, *8*, 1592–1593.

Sellinger, A., & Laine, R. M. (1996b). Silsesquioxanes as synthetic platforms. Thermally curable and photocurable inorganic/organic hybrids. *Macromolecules*, *29*, 2327–2330.

Shin, S. R., Park, S. J., Yoon, S. G., Lee, C. K., Shin, K. M., Gu, B. K., et al. (2006). Anomalous pH actuation of a chitosan/SWNT microfiber hydrogel with improved mechanical property. In E. Comini, P. I. Gouma, V. Guidi, & D. Kubinski (Eds.), *Nanostructured Materials and Hybrid Composites for Gas Sensors and Biomedical applications: Symposium held April 18–20, 2006, San Francisco, California, U.S.A.* (pp. 11–16). Warrendale: Materials Research Society.

Spinks, G. M., Shin, S. R., Wallace, G. G., Whitten, P. G., Kim, S. I., & Kim, S. J. (2006). Mechanical properties of chitosan/CNT microfibers obtained with improved dispersion. *Sensors and Actuators B: Chemical*, *115*, 678–684.

Strachota, A., Tishchenko, G., Matejka, L., & Bleha, M. (2001). Chitosan–oligo(silsesquioxane) blend membranes: Preparation, morphology, and diffusion permeability. *Journal of Inorganic and Organometallic Polymers*, *11*, 165–182.

Strachota, A, Whelan, P., KrÌz, J., Brus, J., Urbanov·, M., Slouf, M., et al. (2007). Formation of nanostructured epoxy networks containing polyhedral oligomeric silsesquioxane (POSS) blocks. *Polymer*, *48*, 3041–3058.

Suchada Boonlertnirun, C. B. a. R. S. (2008). Application of chitosan in rice production. *Journal of Metals Materials and Minerals*, *18*, 47–52.

Tishchenko, G., & Bleha, M. (2005). Diffusion permeability of hybrid chitosan/polyhedral oligomeric silsesquioxanes (POSS(TM)) membranes to amino acids. *Journal of Membrane Science*, *248*, 45–51.

Tiyaboonchai, W. (2003). Chitosan nanoparticles: A promising system for drug delivery. *Naresuan University Journal*, *11*, 51–66.

Song, X. Y., Geng, H. P., & Li, Q. F. (2006). The synthesis and characterization of polystyrene/magnetic polyhedral oligomeric silsesquioxane (POSS) nanocomposites. *Polymer*, *47*, 3049–3056.

Yuchs, S. E., & Carrado, K. A. (1996). A one-step method for the synthesis of a vinyl-containing silsesquioxane and other organolithic macromolecular precursors. *Inorganic Chemistry*, *35*, 261–262.

Zhao, Y., & Schiraldi, D. A. (2005). Thermal and mechanical properties of polyhedral oligomeric silsesquioxane (POSS)/polycarbonate composites. *Polymer*, *46*, 11640–11647.